

## Isolation and Characterization of Cellulose Nanocrystals Created from Recycled Laser Printed Paper

Rogelio Ramírez-Casillas,<sup>a</sup> Karen Fátima Báez-Rodríguez,<sup>a</sup> Ricardo Herbe Cruz-Estrada,<sup>b</sup> Florentina Dávalos-Olivares,<sup>a</sup> Fernando Navarro-Arzate,<sup>a</sup> and Kestur Gundappa Satyanarayana<sup>c,\*</sup>

This article presents the development of a method to prepare nanocrystalline cellulose (NCCs) from laser-printed waste paper using factorial design 2<sup>3</sup> experiments by controlled acid hydrolysis of the waste paper. The method applies high gain ultrasound and subsequent flotation, washing, and bleaching stages. Characterization of the raw material, prepared pulp, test sheets, and NCCs is presented. Optimum conditions to obtain high quality NCCs were found to be 65% acid, for 40 min time of treatment, and residual load in the range of 130 to 570 mmol/kg of NCCs. The obtained NCCs were 80 to 700 nm long depending on the acid hydrolysis conditions. They exhibited high values of whiteness (90.3% Elrepho),  $\alpha$ -cellulose contents (95%), degree of polymerization (731), viscosity (9.59 cP), and chemical compositions similar to that of Whatman paper.

*Keywords:* Laser printing; Waste paper; Environmental safety; Acid hydrolysis; Cellulose nanocrystals

*Contact information:* a: Department of Wood, Cellulose and Paper, “Engineer Karl Augustin Grellmann” University Center of Exact Science and Engineering, University of Guadalajara, Zapopan, Jalisco, 45000, Mexico; b: Center for Scientific Research of Yucatan (CICY), Yucatán, 97205 México; c: Poornaprajna Institute of Scientific Research, Poornaprajnapura, Bidalur Post, Devanahalli, Bengaluru 562110 (Karnataka- India); \*Corresponding author: gundsat42@hotmail.com

### INTRODUCTION

Environmental impacts have reached a critical stage, causing serious consequences to the natural environment all over the world. This is due to the industrial development of great world powers, developing countries, and even third world countries (Alliot *et al.* 2004). With the new age of computer technology and the growth in popularity of personal computers, there has been an increase in the consumption of paper due to all types of printers, including laser printers (Lee *et al.* 2013). It has been reported by the U.S. Environmental Protection Agency that approximately 300 million tons of paper annually are produced all over the world.

The worldwide consumption of paper during the last four decades has increased by 400%, with the USA being the largest consumer of paper (annual consumption of more than 227 kg) (<http://www.thepaperlessproject.com/facts-about-paper-the-impact-of-consumption/>). The same source reveals that during the last two decades, the country's consumption has grown approximately 126% from 92 million tons, with only 5% of world's population represented. According to official figures (Desdelared 2012; Semarnat 2018), Mexico generates an estimated waste of approximately 111,000 tons per day, of which 14% is waste paper. This type of waste paper can certainly impact the environment all over the world and, therefore, there is need for its proper disposal, *i.e.*, recycling and

reuse in some way. Such efforts for the disposal of this waste material in any form (whether as landfill or as a raw material) would have many environmental, economic, and social advantages not only in the USA and Mexico, but also in other countries.

Today, secondary fibers represent an important source of lignocellulosic material for the paper and paperboard industries in developed countries. However, the recycling and reuse of paper presents important challenges for its use due to the aging of fibers, the presence of contaminants (additives used in the manufacturing of the original product, like fillers, adhesives, *etc.*), type of uses such as toner type, injection type, and others, as well as the conditions of use and their final disposal (Monte *et al.* 2012). The removal of non-lignocellulosic materials that adhere to the waste paper and were generated from printing, by cleaning the fibers is done through a process known as deinking. In general, deinking involves several stages: (i) pulping and disintegration, (ii) cleaning and screening, (iii) flotation, (iv) washing, and (v) bleaching (Beneventi 2000).

Of the various stages of the traditional deinking process, the flotation and washing stages have the greatest impact on the elimination of ink from the fibers (Álvarez and Abril 2006). The flotation step is a selective removal of ink particles achieved by the addition of surfactants. The addition of these compounds enables the ink particles to be dispersed, avoiding their deposition on the fiber and favoring their removal from the fiber slurry. It is reported that the speed and efficiency of the flotation process determine the particle size. Therefore, particle sizes outside of the 25  $\mu\text{m}$  to 100  $\mu\text{m}$  range would lead to a decrease in the efficiency of the flotation system (Ramírez *et al.* 2004).

In contrast, during the washing process, a cell is used for the physical removal of the contaminants. In this process, ink particles are dispersed as finely as possible so that they can be removed together with the water and other components through the washing medium. This washing process uses filters with a mesh of approximately 200 threads per inch. It has been reported that washing is effective for particle sizes of 1  $\mu\text{m}$  to 10  $\mu\text{m}$ . For larger particles the washing efficiency decreases considerably, requiring a further series of additional processes such as flotation, purification, or classification (Ramírez 2004; Ramírez *et al.* 2004). It has also been reported that toner inks are difficult to remove by conventional deinking processes as they contain thermoplastic binders that undergo polymerization and fuse onto the paper during the printing process at high temperatures (Ramírez *et al.* 2004). Ink particles involved in printing (toner, ultraviolet (UV), *etc.*) exhibit strong intermolecular cohesion interactions as well as strong bonds with the paper surface, specifically in the fiber. Therefore, they are difficult to separate and, even if it is possible to separate them from paper, they form large platelets, making them extremely difficult to remove with a traditional deinking process (Grossmann *et al.* 2010).

Deinking of laser printing paper has been studied by various researchers using different techniques (Norman *et al.* 1994; Sell and Norman 1995; Tatsumi *et al.* 2000; Gaquere-Parker *et al.* 2009; Pauck *et al.* 2012). Based on these results, it can be said that: (i) the ink particles obtained had a range of sizes depending on the frequency of the generator used with piezoelectric transducers and (ii) ultra sound technique particularly with more stages showed greater efficiency particularly with low consistencies, good recovery of the retention value of water (WRV) of the secondary fiber and near environment temperatures seems to be better method for deinking process which gave better brightness; (iii) low-power, low-gain ultrasound equipment showing limitations of applying to pulps treated in batch processes.

Realizing the fact that large amounts of waste paper are generated globally especially with the use of computers and printing as mentioned above affecting the environment, one of the methods of disposal can be finding new uses for their reuse. However, one possible method is to extract one of the constituents (such as cellulose) from this paper, which is generally produced from fibers with low degree of purity. It should be noted that cellulose is insoluble in most solvents, including strong alkalis, making it difficult to isolate from lignocellulosic materials, as it is intimately bound with lignin and hemicelluloses (Alén 2000). However, in the case of soluble grade cellulose, the fiber is required to have high cellulose content (greater than 90%) and must have very low hemicelluloses, residual lignin, and extractable contents.

The cellulose thus obtained is reported to have very special properties, such as a crystalline arrangement and high levels of whiteness and viscosity (MacDonald 2011). Cellulose, due to its structure, is a compound that has a high potential for use as a nanomaterial, considering its abundance in nature and its nano fibrillar structure. This polysaccharide has very special characteristics that make it an exceptional material, such as its excellent mechanical properties, high rigidity, low cost, and biodegradability (Beck-Candanedo *et al.* 2005). In fact, a number of studies have reported on the production of nanocellulose in the form of crystals using various natural fibers; most such studies used acid hydrolysis as the first digestion method of choice for obtaining the pulp, with organic acids, sulfuric, phosphoric, and hydrochloric acids (Dong *et al.* 1998; Camarero Espinosa *et al.* 2013; Yu *et al.* 2013; Guo *et al.* 2016) in optimum conditions of their concentrations, temperatures, and time. Even oxalic acid has been used at various concentrations (Chen *et al.* 2016) as well as microwave assisted conditions (de Melo *et al.* 2017; Matharu *et al.* 2018). Recently, a review has also been published covering the use of environmentally friendly bio-renewable materials to produce nanocelluloses using different methods and their applications particularly in the form of crystals (Trache *et al.* 2017).

Some of the raw materials from which CNCs can be obtained include a marine animal-tunicate pulp (Samir *et al.* 2004; Samira *et al.* 2008), eucalyptus kraft pulp (BEP) (Beck-Candanedo *et al.* 2005; Wang *et al.* 2014; Chen *et al.* 2016), sisal fibers (Moran *et al.* 2008), and cellulose whiskers from waste from banana rachis (*Musa cavendish*) (Bolio-Lopez *et al.* 2011), sugarcane bagasse (Behin *et al.* 2008; Natthapon *et al.* 2018), softwood kraft pulp (Hamad and Hu 2010), rice straw (Lu *et al.* 2012), recycled pulp (Filson *et al.* 2009; Guo *et al.* 2016), and cotton linter fibres (filter paper) (Lorenz *et al.* 2017).

Regarding waste paper, particularly the laser printed paper, some authors have found that the laser-printed ink particles present on paper are flat. Furthermore, the chemical composition of these particles are functional groups of polymers (polyethylene and polypropylene), which are not very susceptible to chemical treatments. This is because the size of these particles is not reducible; also their adhesion to the paper cannot be easily minimized (Norman *et al.* 1994; Sell and Norman 1995).

Considering the above mentioned facts in respect to finding a new method of disposing waste paper, including that generated with laser printing and the possibility to produce nanomaterials from this waste paper, the main objectives of this study are: (i) to develop a new method to reuse/recycle the waste laser-printed paper and (ii) to characterize the raw material, pulp, and the nanomaterials produced by the waste paper.

In order to meet the other objective to produce nanocellulose crystals (NCCs), a raw material (paper used in laser printing) having high cellulose content (>90%) and very

low content of low removable hemicelluloses was used in this study. Optimum conditions have been arrived to obtain high quality NCCs with chemical composition very similar to standard cellulose. It is hoped that this study will be a forerunner for the utilization of other lignocellulosic wastes generated all over the world.

## EXPERIMENTAL

### Materials

Printed sheets of Maxbrite bond paper (waste laser printed paper) with a letter size of 75 g/m<sup>2</sup> obtained from Office Max, Mexico City, Mexico were used in this study. The characteristics of the original paper used without impression are:  $\alpha$ -cellulose of 84.2%,  $\beta$ -cellulose of 12.6%,  $\gamma$ -cellulose of 3.2%, whiteness of 87.7%, and values of  $L^*$ ,  $a^*$ , and  $b^*$  being 95.0, 0.1 and 0.1, respectively. It may be noted that  $L^*$  represents the lightness of different colors, starting from from zero for black to 100 for perfect white;  $a^*$  represents a red color when the number is positive, green when it is negative, and zero when it is grey. Finally,  $b^*$  represents a yellow color when positive, blue color when it is negative, and is zero for grey as per TAPPI T 527 om-94 (1994).

### Methodology

A number of steps were involved in obtaining nanocrystals of cellulose using the printed paper (waste paper). These are shown schematically in Fig. 1.

To homogenize the amount of toner deposited on each sheet, sheets of bond paper were printed on one side with the following legend: "Deinking of printing paper Laser, applying sequences with ultrasound of intensive action, oriented towards the obtaining of cellulose of high purity", using a laser printer (Make: Hewlett Packard; Model: HP Laser Jet 1022, México City, México). In fact, it is proper to use HP Laser Jet 1022 toner cartridge with the selected paper. The characteristics of the toner used are: styrene acrylate copolymer 55 to 65%, iron oxide 30 to 40%, and salicylic acid chromium chelate 1 to 3%. The specified test was repeated several times, until a total of 45 rows were filled. The text was printed in the Times New Roman font (size 12), bolded, and double spaced. This allowed for the deposit of an approximate amount of 0.1872 g of toner/sheet.

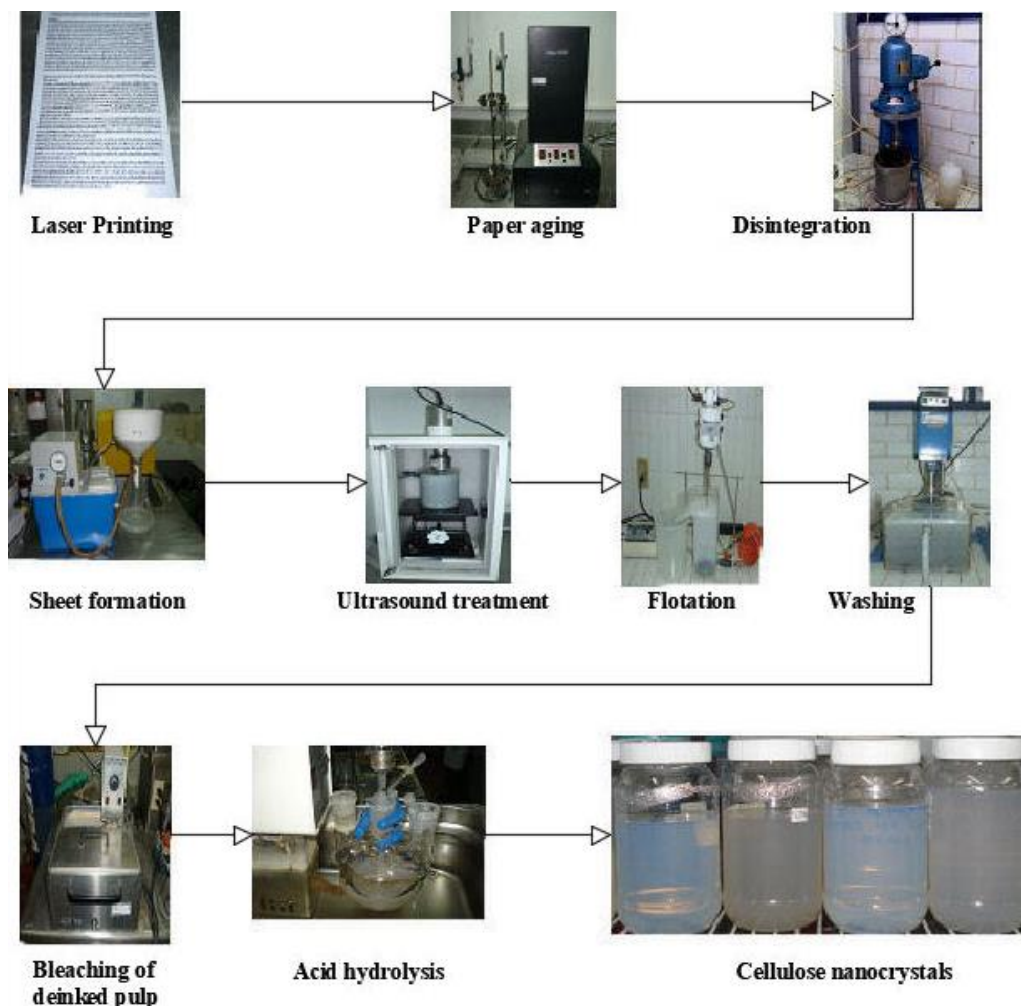


**Fig. 1.** Schematic diagram of steps involved in the preparation of cellulose nanocrystals *Printing with laser technology*

#### *Aging of sheets of laser bonded paper*

Following an earlier report stating that the toner particles freshly deposited onto paper by laser printing do not exhibit sufficient adhesion compared to the waste paper stored for a long time (Ramírez Valdovinos 2013), the printed sheets of paper used for this study were subjected to an aging process. This was done by exposing the paper to UV light for 60 min to promote a better adhesion of the toner particles on the bond paper and to simulate the characteristics of laser-printed waste paper with a longer storage time. A Rayonet make photo-reactor (Model RPR-100, manufactured in The Southern New England Ultraviolet Co., Branford, CT, USA) was used for this with 350 nm wavelength lamps and an 8-compartment rotating carousel, where the paper was held during accelerated aging for 60 minutes.

#### *Disintegration*

Following Technical Association of the Pulp and Paper Industry (TAPPI) T205 SP-95 standard (1995), the above laser-printed waste paper was subjected to a disintegration process at 1.2% consistency for 5 min in a Frank disintegrator (Karl Frank, Type 95967, manufactured in Hamburg, Germany) with a rotating speed of 3000 rpm.

### *Formation of test sheets*

After each step, from the disintegration step to the washing step, test sheets were formed to check the amount and size of the ink particles that were present in each sheet and, thus, the ink removal of the laser-printed sheets.

Sheets of 130 g/m<sup>2</sup> were prepared in the laboratory according to the TAPPI T218 sp-11 standard (2011). Sheet formation was performed in a porcelain Buchner funnel of 20 cm in diameter, using a Whatman No. 6 filter paper base with a pore diameter of 3 µm. Each sheet was placed in wooden frames (as a tension medium) and air dried for a period of 24 h. The sheets derived from the fibrous slurry, which was obtained during the disintegration steps, were considered as the control targets.

### *Ultrasound treatment*

After the sheet formation, the paper was subjected to an ultrasound treatment for separation into fiber suspension. This process does not damage the fibers and followed the conditions reported earlier (Ramírez Valdovinos 2013). For this purpose, a Sonics ultrasonic processor VCX-750, manufactured by Sonics & Materials, Inc., Newtown, CT, USA was used with a working frequency of 25 kHz, power of 400 W, and a solid type probe of high gain of 2.5 cm dia, part No. 603-0209, having low intensity, volume (batch) 100 to 1000 mL, amplitude 35 µm and 122 mm length. The optimized values used for this treatment were a 20 min treatment time, 0.5% slurry consistency, and a 25 °C slurry temperature, the latter being controlled close to 25 °C by using a cooling system fabricated in the authors' department coupled to the ultrasonic processor.

### *Flotation stage*

Following an earlier report (Ramírez Valdovinos 2013), the slurry was subjected to a flotation process in a Barnant Mixer cell using two surfactants, commercial ISTEMUL 780 at 0.1% and sodium-4-polystyrene sulfonate (obtained from RG Laboratories, Guadalajara, Jalisco, Mexico) at 0.9% dry paper basis with operating conditions specified according to the PTS-RH010/87 (1987) method. The operating conditions used were an air supply of 60 L, agitator speed of 1500 rpm, flotation time 10 min, and a consistency of 0.80%.

### *Washing step*

The fibrous suspension obtained in the previous step was then subjected to a washing sequence using conditions reported earlier (Ramírez Valdovinos 2013) with a Degussa cell manufactured in Frankfort, Germany with 200-mesh wash for 10 min, a water flow of 1 L/min, and a consistency of 0.4%.

### *Bleaching of deinked pulp*

With the goal of increasing the  $\alpha$ -cellulose content and degree of brightness (whiteness) of soluble grade cellulose (ISO 11475:2004), the pulp was then bleached. This resulted in brightness (whiteness) above 90° and  $\alpha$ -cellulose content between 90% and 96% in the pulp after the process of deinking with high gain ultrasound. In contrast, the main objective was to obtain NCCs from the pulp of laser printing paper by subjecting it to an ECF bleaching process. The conditions used for this process are listed in Table 1.

**Table 1.** Parameters Used for ECF Bleaching

Control Parameter	Step I	Step II	Step III	Step IV
	Chlorine Dioxide (ClO <sub>2</sub> )	Hot Extraction (NaOH)	Chlorine Dioxide (ClO <sub>2</sub> )	Cold Extraction (NaOH)
Temperature (°C)	70	70	80	30
Time (min)	60	60	180	60
Consistency (%)	10	10	10	10
ClO <sub>2</sub> (%) #	Kappa No. x 0.24	-	2.5	-
NaOH (%) #	-	$\left[ \frac{\%R_1 ClO_2}{2} \right] + 0.2$	-	10

#: Percentages of the reagents with respect to dry fiber grains.

It is noted that Kappa number, which is the volume (in mL) of 0.1 N potassium permanganate solution consumed by one gram of moisture-free pulp under the specified conditions, was determined following TAPPI T 236 cm-85 standard. This can be used for all types and grades of pulp (chemical, semi-chemical, unbleached and bleached) to get yields below 60%. It is also possible to use this method to evaluate pulps with 70% yield if one uses screened pulps. Accordingly, in this study this number was obtained and the results are corrected to 50 % of the added permanganate solution.

#### Obtaining NCCs

Finally, the bleached pulp was subjected to controlled acid hydrolysis with sulfuric acid to obtain cellulose nanocrystal suspensions under various acid concentrations, treatment times, and system temperatures. For this purpose, the 2k multi factorial experimental design was followed with several experiments. While Table 2(a) summarizes the various parameters and applied conditions, Table 2(b) gives details of the variables used in different experiments. After each experiment, suspensions of NCCs were purified, labeled, and stored at a low temperature (4 °C). A solution with a 10:1 ratio of hydromodule to sulfuric acid was left over in dry base pulp as a fixed parameter along with a constant stirring speed of 300 rpm.

**Table 2(a).** Parameters and Conditions Used in the Production of NCCs from Purified Cellulose, Obtained from Laser Printed Office Waste Paper

Design 2 <sup>3</sup>		
Variables	Low Limit	High Limit
Time (min)	40	70
Temperature (°C)	40	60
Concentration of acid (%)	60	65

**Table 2(b).** Parameters and Experimental Conditions Applied During the Acid Hydrolysis of the Bleached Pulp Obtained from the High-gain Ultrasonic Deinking of Laser Printed Waste Paper

Experiment No.		Parameters		
No.	Concentration of H <sub>2</sub> SO <sub>4</sub> (%)	Temperature (°C)	Time of treatment (min)	
1	60	40	40	
2	65	40	40	
3	60	60	40	
4	65	60	40	
5	60	40	70	
6	65	40	70	
7	60	60	70	
8	65	60	70	
9	62.5	50	55	
10	62.5	50	55	

Finally, with the goal of knowing the amount of sulphate groups (in mMol/kg of NCCs) grafted onto nanocrystals as a response variable, the residual concentration of ionizable groups on the surface of the nanocrystals (in mMol/kg of NCCs) and the average particle size of the NCCs was considered.

Variance analysis with a general linear model was performed with a 95% confidence level ( $P < 0.005$ ) using the Statgraphics statistical program (Statgraphics Centurion V. 16.1.11, The Plains, Virginia, USA) to find the significant factors that influenced the residual concentration of ionizable groups on the surface of the nanocrystals (in mmol/kg of NCCs) and the average particle size of the NCCs. The factors thus evaluated included: concentration of sulfuric acid (A), and the temperature (B) and time of treatment (C). Statistical F tests, analysis of variance (ANOVA), were used to obtain the probability (P).

#### *Characterization of the raw material, prepared pulp, and test sheets*

Following the standards established by TAPPI, whiteness and opacity of the original bond paper samples used for preparing the NCCs as well as laboratory prepared paper sheets were evaluated using an Elrepho 3000 spectrophotometer (Datacolor, New Jersey, USA). The standards used for optical properties and color of both samples were TAPPI T452 om-08 (2008) and TAPPI T527 om-07 (2007), respectively. Measurements were made on all the NCCs obtained in all stages of the experimental design with five repetitions made at each stage of the experimental design, including for each determination of its constituents. The nanocrystals obtained were of the whisker type. It is reported that the particle type of crystals in general is elongated and flat having dimensions of a few hundreds of nanometers long, 10 to 20 nm wide, and a few nm thick [Samira *et al.* 2008]. There are also reports of obtaining whisker-like crystals having typical diameters of 5 to 50 nm, lengths of 100 to 3000 nm through controlled hydrolysis with mineral acids (Araki *et al.* 2001; De Souza Lima *et al.* 2002; Šturcová *et al.* 2005).

For the determination of the chemical compositions of the prepared NCCs, approximately 20 mL of samples were placed in an oven for drying to obtain NCCs films. Therefore, solid samples obtained from NCCs were analyzed using a Perkin Elmer

Fourier Transform Infrared Spectrophotometer (FTIR) (Spectrum GX, Perkin Elmer, Mexico City, Mexico) using an attenuated total reflectance diamond crystal tip (ATR).

In addition,  $\alpha$ ,  $\beta$ , and  $\gamma$ -cellulose contents of both the papers were also determined following the standard TAPPI T203 om-93 (1993). The degree of polymerization of the cellulose obtained was also determined by viscosity tests. Similarly, the bleached pulp was analyzed for whiteness following the ISO whiteness standard (11475: 2004), and  $\alpha$ ,  $\beta$ , and  $\gamma$ -cellulose contents were determined following TAPPI T203 om-93 (1993) with the aim of using high-quality  $\alpha$ -cellulose for the production of nanocrystals.

The viscosity and degree of polymerization (GP) of the original bond paper and that after the bleaching process were determined, as these were essential for any soluble grade type pulp. In fact, its value is supposed to be a minimum of 500 (MacDonald 2011; Testova *et al.* 2014).

#### *Characterization of nanocellulose crystals*

Nanocrystal suspensions were characterized for particle size distribution, chemical composition, and residual charge. Particle size distribution was evaluated by dynamic laser light scattering (DLS) (Make: Malvern, Worcestershire, United Kingdom) and atomic force microscopy (AFM) instruments (Park Systems Inc., Suwan, South Korea).

The DLS is widely used for the measurement of nanoparticle size. This is mainly because it is relatively cheap and convenient for measuring size distributions. DLS does not measure the particle size directly as AFM does or any other type of microscopy. It measures the Brownian motion of the nanoparticles in suspension by measuring the fluctuation of the intensity of the light scattered from the particles and relates it to the diffusion coefficient and the size of the particles.

For the above measurement purposes, the suspensions of NCCs were first diluted to 0.2% v/v and filtered using a syringe filter of 25 mm in diameter and 1.6  $\mu\text{m}$  pore size. Subsequently, the samples were sonicated in an Elma ultrasonic bath with a frequency of 20 kHz for 5 min. Finally, the suspensions of NCCs were placed in a polypropylene cell and analyzed with a Zetasizer Nano instrument (Make: Malvern, Worcestershire, United Kingdom) using the defined operating procedure described in the previous part for the analysis of NCCs.

The morphology of NCCs was studied using Park systems AFM equipment (Model NX-10-Park Systems Inc, Suwan, South Korea) by obtaining micrographs of different sizes (5  $\mu\text{m} \times 5 \mu\text{m}$ , 2.5  $\mu\text{m} \times 2.5 \mu\text{m}$ , and 1  $\mu\text{m} \times 1 \mu\text{m}$ ), using budget microchip sensors (Model: TAP-300-G (Park Systems Inc, Suwan, South Korea) attached with the AFM. The images were obtained at a resolution of 512  $\times$  512 lines, using the technique of intermittent contact in air. Images of the prepared NCCs particles under some of the hydrolysis conditions were obtained in order to have intermediate patterns for comparison.

It may be noted that for the determination of the length, diameter, and thickness of NCCs (obtained as suspension), it is necessary to separate the nanocrystals in such a way that each nanocrystal is separated from all the others in an independent way. Accordingly, up to 10 measurements were made for each experiment, and these measured dimensions were averaged.

For the determination of the chemical compositions of prepared NCCs, approximately 20 mL of samples were placed in an oven and dried to obtain NCC films. Thus, obtained solid samples of NCCs were analyzed using a Perkin Elmer Fourier

transform infrared (FTIR) spectrophotometer (Spectrum GX, Perkin Elmer, Mexico City, Mexico) using attenuated total reflectance (ATR) with crystal diameters. Spectra were obtained from three different points of the sample with 16 scans in the range of  $4000\text{ cm}^{-1}$  to  $500\text{ cm}^{-1}$  with a resolution of  $4.00\text{ cm}^{-1}$  to ensure that the obtained spectra were representative of their samples.

Finally, residual charge (load) in the NCC suspensions was determined by conductometric analysis. For this purpose, 0.05 N NaOH solutions were taken in a digital burette. This, along with a three-necked flask containing a pH electrode and a conductivity electrode (Orion Star A211 pH meter; Thermo Fischer, Massachusetts, USA), were coupled to a laptop to record the volume of added soda (NaOH) and the corresponding pH and conductivity values (mS/cm). All evaluations were conducted in an argon environment to avoid absorption of  $\text{CO}_2$  during the analysis.

## RESULTS AND DISCUSSION

### Brightness (whiteness) and Cellulose-related Contents

It is reported that prepared dissolving pulps would have some special characteristics such as high content of  $\alpha$ -cellulose (91 to 95%), high brightness (>90%) indicating high purity of the pulp, low contents of hemicelluloses (1 to 5%) lignin (<0.5%) besides very low levels of minerals (0.1%) (Sixta 2006). In addition, there are two more parameters to be considered. These are degree of polymerization (DP) of the cellulose chains and viscosity of the pulps, which usually indirectly monitors the former.

Table 3 shows obtained values of the whiteness and cellulose contents, which presents the purity of pulp and cellulose in this study.

**Table 3.** Comparison of Properties of the Deinked Pulp and the Bleached Pulp

Parameter	Characterization of Pulps			
	Unbleached Fiber (Deinked Fiber)	Standard Deviation	Bleached Fiber	Standard Deviation
Whiteness ISO (%)	84.40	0.111	90.30	0.111
$L^*$	93.94	0.019	96.31	0.073
$a^*$	-0.26	0.011	-0.002	0.0014
$b^*$	0.64	0.011	0.42	0.011
$\alpha$ -Cellulose (%)	84.24	0.115	94.97	0.065
$\beta$ -Cellulose (%)	7.41	0.085	2.36	0.073
$\gamma$ -Cellulose (%)	8.35	0.074	2.67	0.077

It can be seen from the Table 3 that  $\alpha$ -cellulose content of the bleached pulp was about 95%, while that of unbleached pulp was about 90%, indicating the purity of the obtained cellulose after bleaching and suggesting that bleaching could remove elemental chlorine from the unbleached pulp. This value of  $\alpha$ -cellulose of bleached pulp is similar to the earlier reported value obtained in sugarcane bagasse (Behin *et al.* 2008), while it is

slightly higher than the other recently reported value of about 91% (Natthapong *et al.* 2018). In the case of color of the bleached pulp, although the value of brightness of bleached pulp was about 90%, pulp showed a slightly bluish tinge. This is understandable from the obtained low values of  $a^*$  and  $b^*$  values of the bleached pulp shown in the above table. However, all the values shown in the above table indicate that the starting materials met the requirements of dissolving grade cellulose.

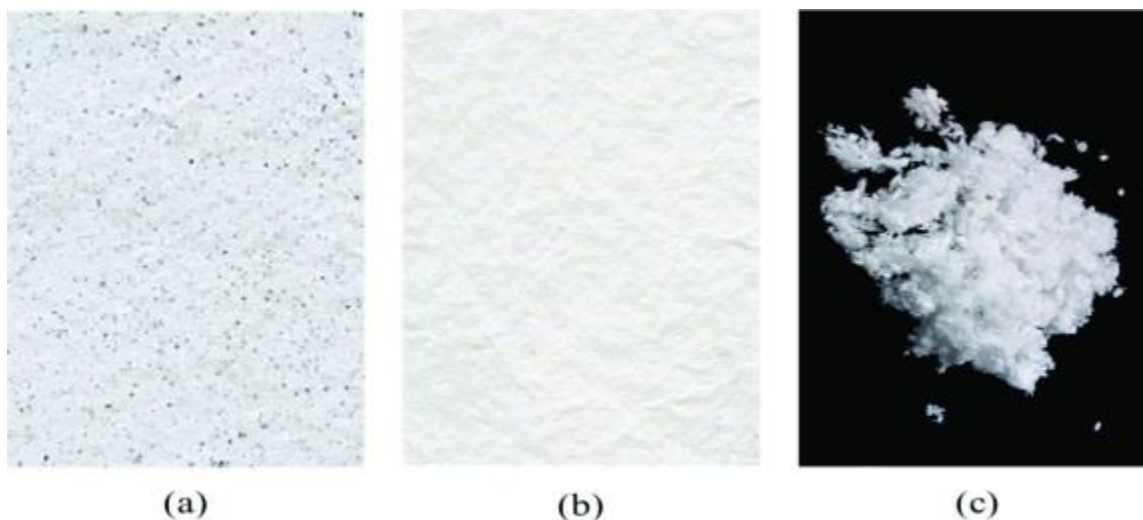


**Fig. 2.** Photographs of the appearance of the pulp in different stages: (a) disintegration, (b) deinking, and (c) ECF bleaching

The appearance of the bleached pulp compared to the pulps obtained prior to and at the end of the deinking process are shown in Fig. 2, wherein Fig. 2a shows disintegrated pulp (before treatment with ultrasound), Fig. 2b shows that after ultrasound treatment (deinking), and Fig. 2c shows the pulp after bleaching. As shown, the bleached pulp/fiber had a less-yellow color than the other two and very few ink particles.

### Degree of Polymerization and Viscosity of the Obtained Cellulose

Table 4 shows the values of the degrees of polymerization of the deinked pulp and bleached pulps of 0.15 g. The observed value of degree of polymerization in this study is comparable to that earlier reported value of 780 (Behin *et al.* 2008). It is also interesting to see that the final pulp obtained after 3 and 4 stages of bleaching reached higher DPs (723.1 and 731.3) compared to the de-pulped sample (634.7). This could be due to the fact that the initial pulp contained fines and, when this pulp was subjected to successive chemical processes designed to dissolve the cellulose (this is a method to determine the degree of polymerization is dissolving cellulose), cleaning of the pulp would have been carried out, resulting in the removal of the fines present in it.

It may be noted that it was necessary to remove the fines of cellulose from the raw material before determining the degree of polymerization. This is justified by looking to Table 4, which shows the properties of cellulose at different stages of bleaching. Thus it may be said that it is desirable that the base raw material for the production of the NCCs should not contain very short fibers (termed as ‘fines’), which could initiate a degradation of the fibrous material.

**Table 4.** Properties of the Cellulose in Different Stages of Bleaching

Sample	Degree of Polymerization	Viscosity (cp)
Deinked pulp	634.68	8.14
Bleached pulp in 3 stages	723.07	9.56
Bleached pulp in 4 stages	731.34	9.59

With MCC, when the starting material has been already hydrolyzed to LOPD, the same reaction setting has been used in sulfate esterification, but the yield has been only 20 to 30% (Araki *et al.* 1999; Bondeson *et al.* 2006). This provides a warning that there may be problems in the dispersion. High CNC yields (\*90% or higher), however, have been achieved when hydrolyzing the fibers without any mechanical treatment and then applying whole hydrolyzed fibers in the dispersion step with sonication (Kontturi *et al.* 2016) or when using new kinds of mechanical approaches (Yu *et al.* 2013; Chen *et al.* 2016).

### Yield of NCCs

The yield of nanocrystals obtained is considered to be an important issue related to the production of NCCs (Hamad and Hu 2010; Chen *et al.* 2015; Guo *et al.* 2016; Kontturi *et al.* 2016; Lorenz *et al.* 2017; Salminen *et al.* 2017). Wang *et al.* (2014) stated that two key processes dictate the yield of NCCs, the first being depolymerization of cellulose under low-severity conditions, *e.g.*: acid concentrations of <58 wt. %, and the second being degradation of NCCs at very high-severity conditions (acid concentrations of  $\geq$  64 wt. %).

**Table 5.** Source, Preparation method, Yield, and Dimensions of Nano Cellulose Crystals

Source	Preparation Method	Yield (Wt. %)	Dimensions (nm) Length; Dia/Width/ Thickness	Reference
Laser printed paper	Acid hydrolysis	38	80-700 800 100-400 (Bimodal); 100 (Unimodal)	Present Study
Filter paper whatman No. 1	Acid hydrolysis	43.5	177-390	Dong <i>et al.</i> 1998
Eucalyptus Kraft pulp Wood*	Acid hydrolysis	NK	147 nm 100-300 ; 3-5	Beck-Candanedo <i>et al.</i> 2005
Tunicate*		-	100-several $\mu\text{m}$ ; 10-20 nm	*- Adopted from above
Bacterial*		-	100-several $\mu\text{m}$ ; 5-10 by 30-50	
Algal (Valonia)*		-	>1000; 10 to 20 nm	
Cotton*		-	200-350; 5 nm	
Avicel, Cotton and tunicin	Acid hydrolysis	NK	105-141 (Cotton/Avicil) 1073 (tunicin)	Samira 2008
Recycled pulp	Enzymatic	4.9-38 (Microwave heating); 3.4-29 (Conventional heating)	100-1800; 30-80	Filson <i>et al.</i> 2009
Eucalyptus kraft pulp	Bleached with Glucan	70	NA	Chen <i>et al.</i> 2015
Eucalyptus kraft pulp	Hydrolysis using organic acid	75	275-380	Chen <i>et al.</i> 2016
Orange peel residues	conventional acid hydrolysis and acid-free microwave processing	30-50	(3–15 $\times$ 500–2000 nm)[HT: 120-200 $^{\circ}\text{C}$ ]; (3–15 $\times$ 500–2000 nm [HT: 180 $^{\circ}\text{C}$ ]; NCCs: (200–400 $\times$ 40–50 nm) and crystallites (5–15 $\times$ 40–50 nm) [Beyond 180 $^{\circ}\text{C}$ and selective leaching/hydrolysis of amorphous regions].	De Melo <i>et al.</i> 2017
Citrus Cellulosic matter	Acid-free microwave-assisted selective scissoring	25-72	NA	Matharu <i>et al.</i> 2018
Cellulose raw materials	Hydrothermal conditions	93.7	NA	Yu <i>et al.</i> 2013

NA: Not Available

It is reported that the yield of NCCs with conventional sulfuric acid hydrolysis ranges between 10 and 80%, strongly depending on the hydrolysis conditions (Hamad and Hu 2010; Hu *et al.* 2014; Wang *et al.* 2014; Chen *et al.* 2015; Guo *et al.* 2016). It is also reported that low values of yield depend not only on the extensive hydrolysis of cellulose into soluble sugars as normally speculated by many researchers, but also on the strength of sonication that is used to break some of the fiber fragments (Salminen *et al.* 2017). In fact, it is reported that exceptionally high yields of NCCs are possible by using acid vapor (Kontturi *et al.* 2016; Lorenz *et al.* 2017) or hydrolysis of the cellulosic materials without any mechanical treatment followed by sonification of these hydrolyzed materials during the dispersion step (Kontturi *et al.* 2016) or resorting to new types of mechanical approaches (Yu *et al.* 2013; Chen *et al.* 2016). In fact, Yu *et al.* (2013) have observed that about 94% yield of thermally stable NCCs by using combination of hydrothermal hydrolysis and neutralization of HCl using ammonia, which can then be removed by simple heating.

The yield obtained in the present study was found to be 38 wt. %. Table 5 lists the comparison of value of yield, dimensions of NCCs obtained in the present study with the earlier reported values these two characteristics of NCCs by various researchers using different types of natural cellulose raw materials and different processing conditions. It can be seen that the yield value obtained in the present study is comparable with many of the reported values.

### Light Scattering Studies of NCCs

Figure 3 shows the results of laser light scattering measurement of the size of NCCs obtained from laser light scattering measurements made using the Zetasizer equipment. These values were obtained from several of the factorial designed acid hydrolysis experiments as listed in Tables 2a and 2b. Table 5 lists sizes of NCCs obtained in this study along with earlier reported values from different sources and preparation methods.

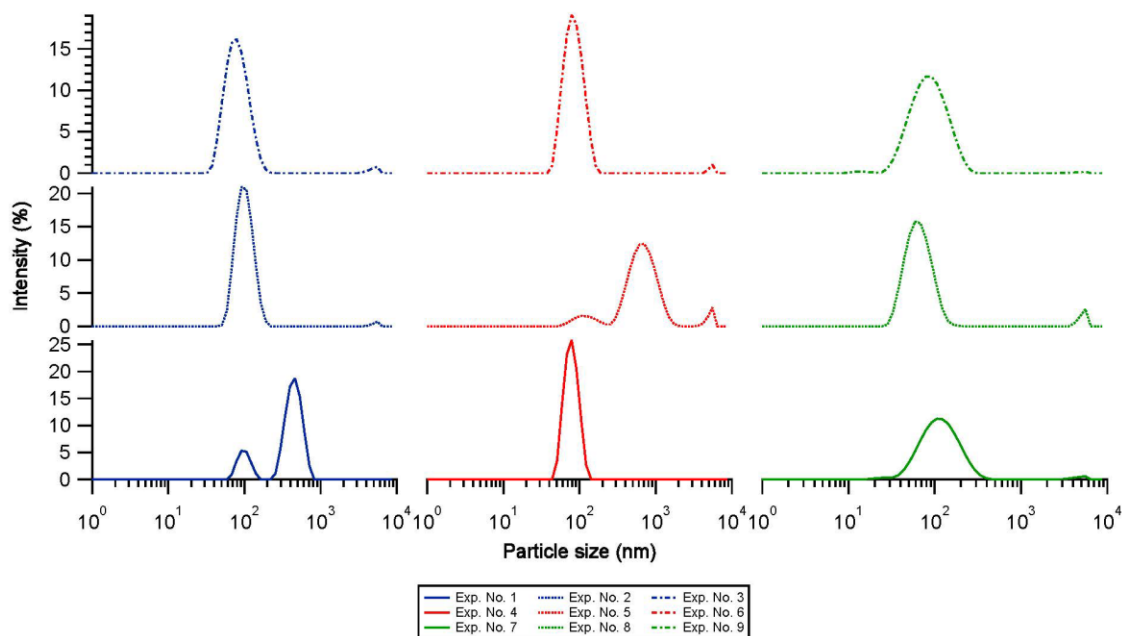


**Fig. 3.** Results of laser light scattering measurement of the size of NCCs

It can be seen from the graphs that experiment number 7 showed a Gaussian type A unimodal pattern. In the case of experiments 2, 3, 4, and 6, maximum sizes of NCCs were obtained below 100 nm, while the average size of the NCCs was greater than 100 nm in experiments 7, 9, and 10, which also showed a greater variation in size distribution.

In contrast, bimodal patterns can be seen in experiments 1 and 5, suggesting that, under the used experimental conditions, it was possible to produce NCCs with different morphologies. The particles obtained under these conditions exhibited NCCs with an average size close to 100 nm, although there were particles larger than 400 nm. These bimodal patterns and the particle sizes obtained are quite interesting due to the fact that this may be the first report of such a result. This may have been due to the fact that the fibrous material used as the starting material could have been a mixture of long fibers, short fibers, and mechanical pulp, as observed in the microscopic analysis. This analysis is found to be enough, since the raw material as observed showed a mixture of materials as mentioned above. In fact, as can be seen from Fig. 2, the hydrolysis of the cellulose resulted in the generation of NCCs with different morphologies under the experimental conditions used in this study.

It is also interesting to note the reported results of size of obtained NCCs by other researchers for comparable with those observed in the present study. Shorter hydrolysis time has yielded large size (177 to 390 nm) NCCs (Dong *et al.* 1998).

On the other hand, NCCs of length 275-380 nm have been reported in the new advances in the synthesis of NCCs, which include organic acids processing and microwave-assisted conditions (Chen *et al.* 2016; Bian *et al.* 2017; Matharu *et al.* 2018). Another new method of recycling of NCCs by enzymatic process have resulted NCCs of varying lengths of 30 to 80 nm in width and lengths of 100 to 1800 nm (Filson *et al.* 2009).

As mentioned earlier, one should use low concentration of acid and temperature to get NCCs of larger lengths, which is in agreement with earlier reported results (Chen *et al.* 2015). It may be noted that under the used experimental conditions in this study, the hydrolysis of cellulose was not so severe, which would have allowed for the generation of NCCs with marked morphological differences as those in the present study.

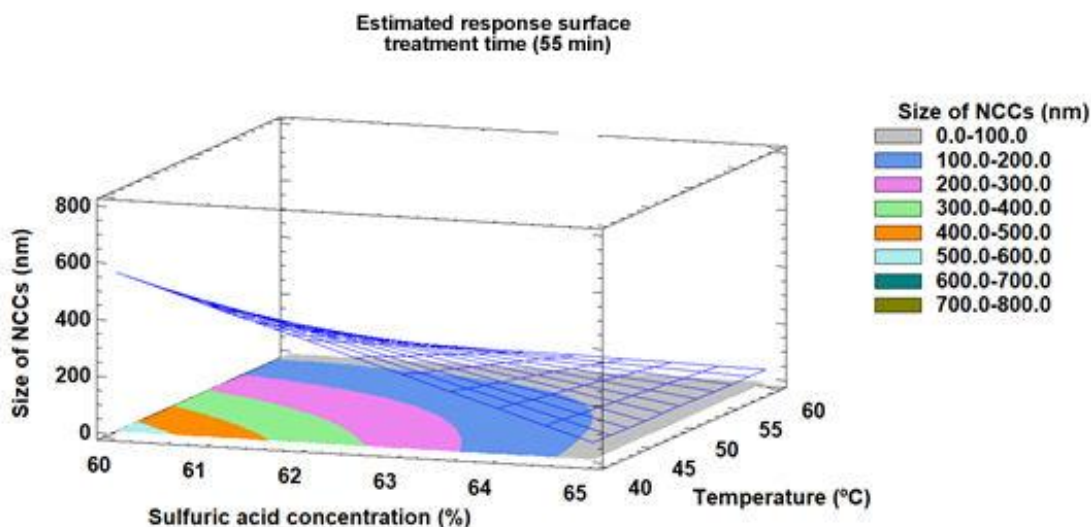


**Fig. 4.** Response surface of the size analysis of NCCs obtained under various acid hydrolysis conditions controlled with H<sub>2</sub>SO<sub>4</sub>. (Factors: Concentration of acid vs temperature)

With the data obtained from the averages of the distribution curves of the sizes of the NCCs, evaluated by DLS, a statistical analysis was performed. Based on the above analysis, a response surface plot was obtained, which is shown in Fig. 4, taking into account the statistically significant factors.

Figure 4 shows that to achieve NCCs with large dimensions, one would have to use low concentrations of H<sub>2</sub>SO<sub>4</sub> and low temperatures (40 °C). Another relevant issue was the fact that, according to the chart, temperature had no significant effect (in the range evaluated) when an acid concentration of 65% was used.

Based on the appearance of the NCCs in Fig. 4, in order to obtain NCCs with large lengths (nm), it is necessary to work at low acid concentration (60%), low temperature (40°C). On the other hand, when working at high acid concentrations (65%), results in Fig. 4 indicate no significant effect of temperature in the range of 40 and 60 °C.

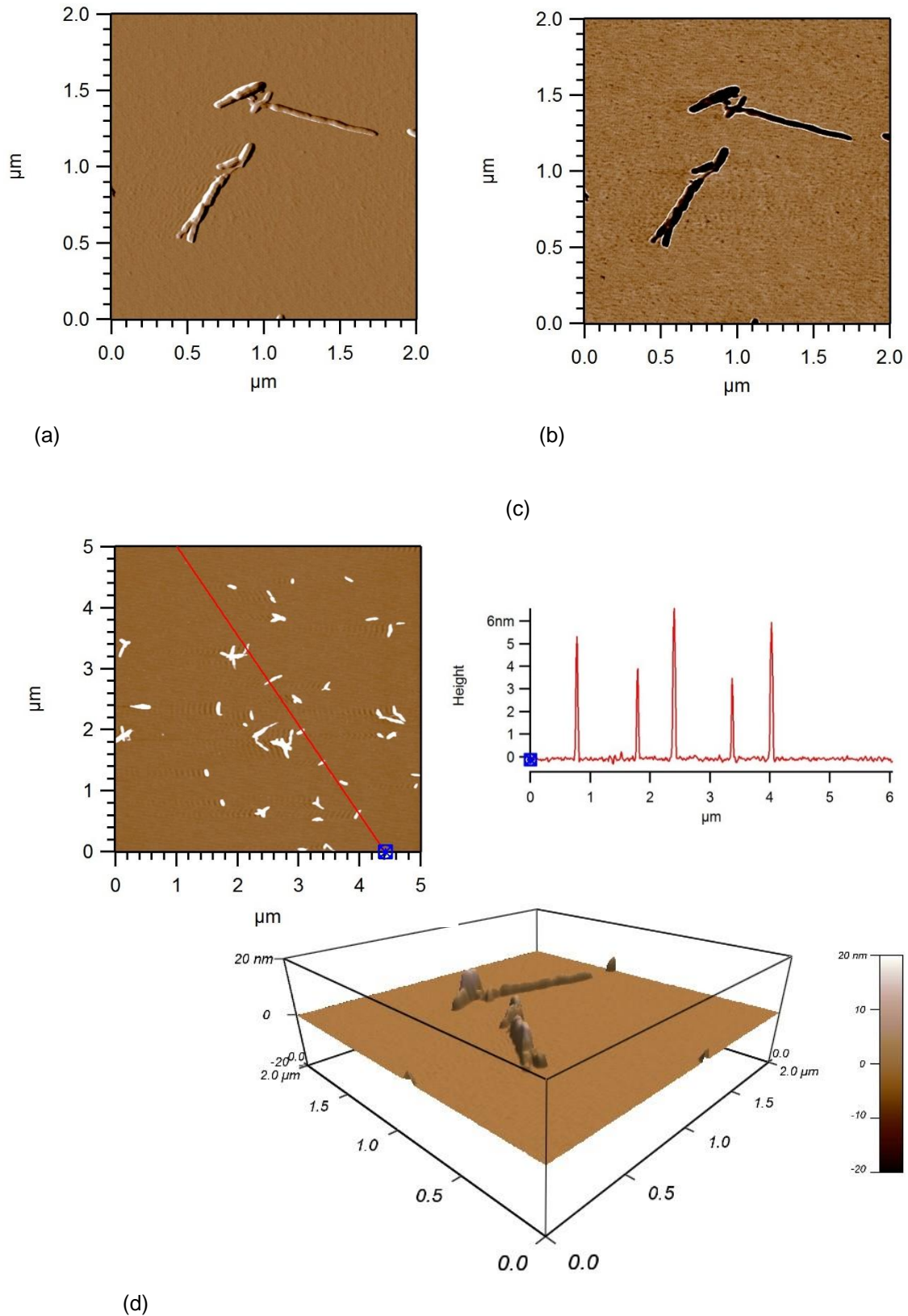
### Morphology Studies of NCCs

Figure 5 shows the AFM micrographs of the NCCs obtained under the conditions of experiment number 1.

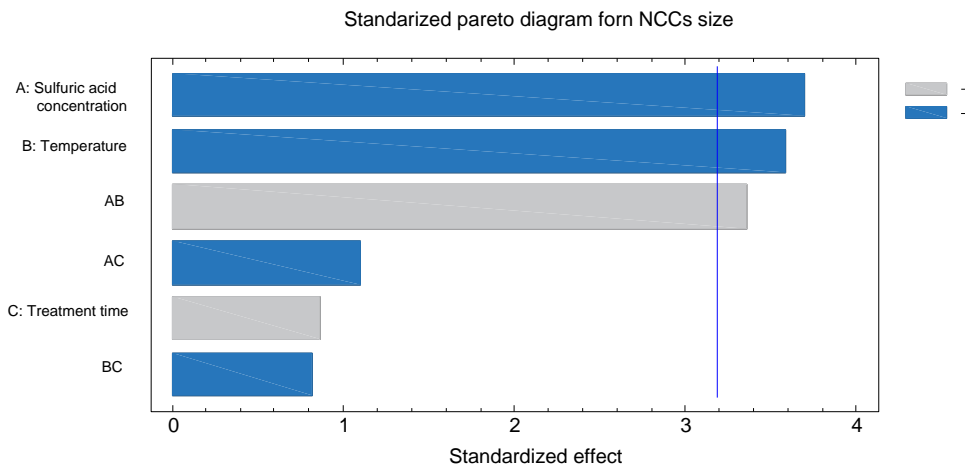
Figure 5(a) shows the amplitude image indicating the presence of very long (approximately 800 nm) but thin NCCs, along with particles approximately 100 nm in length, but of a more robust appearance. In contrast, Fig. 5(b) shows the phase image suggesting that AFM could reveal only two distinguished materials, one with dark appearance, corresponding to the NCCs, and another with a lighter (clear) appearance corresponding to the substrate. Therefore, from the above it may be inferred that under the experimental conditions used, no waste was generated other than obtained NCCs as reported elsewhere (Filson *et al.* 2009; Chen *et al.* 2016, 2017; Matharu *et al.* 2018).

Figure 5(c) shows the 3D projection of these particles, which suggests that the height of the NCCs was variable. Finally, Fig. 5(d) shows the plot obtained by performing a section analysis (red line) of an image taken in an area of 5 μm × 5 μm. From this, it was seen that the NCCs had a thickness of approximately 4 nm to approximately 6 nm. These results confirmed the assumption made earlier in the DLS analysis of samples obtained from these experimental conditions, where a bimodal pattern was found in the size distribution of NCCs. To justify this statement, a statistical analysis was carried out with the data obtained from the distribution curves of the sizes of NCCs, evaluated by DLS analysis, which had taken into account the statistically significant factors. In fact, as mentioned earlier, Fig. 4 represents a surface graph, which indicates that one should use low concentration of acid and temperature of 40 °C to get NCCs of larger lengths. This also suggests that the temperature did not have a significant effect in the range evaluated when an acid concentration of 65% was used.

Further, it may be noted that an experimental design was made in this study considering all the relevant variables and then attempted to arrive at the variables of greatest influence. This is illustrated in a Pareto diagram (Fig. 6) with factors of greater influence in the generation of the particle size of NCCs, under various conditions of controlled acid hydrolysis. Accordingly, it was observed that concentration of acid used and the temperature were of greatest influence. According to this design, only the AFM images of experiment 1 are shown, which gave the NCCs having larger lengths, while NCCs of shorter lengths were obtained in experiment 3.



**Fig. 5.** The AFM analysis images of NCCs obtained from experiment number 1, (a) amplitude, (b) phase, (c) 3D projection, and (d) section analysis graph



**Fig. 6.** Pareto diagram with factors of greater influence on the generation of the particle size of NCCs, under various conditions of controlled acid hydrolysis

Figure 7 shows the results obtained under the conditions of experiment number 3. Parts a and b of Fig. 7 show the AFM images of obtained NCCs in this experiment, which revealed the morphologies in the conditions of the experiment wherein a larger number of NCCs per area can be seen besides some agglomerations. The smaller size and more homogeneous distribution of the NCCs in these compared to those observed in Fig. 5 are evident in this figure. This was in agreement with the corresponding DLS analysis presented earlier.

In addition, phase analysis indicated that, in the case of experiment number 1, only NCCs were deposited onto the surface of the mica, which suggested that, under the conditions of the applied hydrolysis, no residues were detected, indicating excessive degradation of the obtained cellulose. The section graph (Fig. 6d) indicated that the thickness of the NCCs, under the conditions of the applied hydrolysis, ranged from 4 nm to 6 nm. This distribution of particle size and morphology of the NCCs were similar to those reported earlier by Jonoobi, Hossain, Roman, and their coworkers (Roman and Winter 2004; Jonoobi *et al.* 2010; Hossain *et al.* 2012).

### Chemical Composition of NCCs

The infrared spectra of the NCC films obtained by FTIR ATR are shown in Fig. 8, which revealed small differences between the various samples analyzed.

It may be noted that C-2 to C8 represent samples from different experiments. It can be seen that the band appearing in the region of  $3300\text{ cm}^{-1}$  to  $3400\text{ cm}^{-1}$  is characteristic of hydroxyl groups belonging to the cellulose. Other bands that lie in the region  $2850\text{ cm}^{-1}$  to  $2900\text{ cm}^{-1}$  and  $1400\text{ cm}^{-1}$  were attributed to the stretching of the C-H groups. Another band between  $1600\text{ cm}^{-1}$  corresponded to stretching of the O-H groups in the structure of the nanocrystals. Other bands observed in the spectra were typical of cellulose, due to its COC-type asymmetric vibrations. The bands at  $1100\text{ cm}^{-1}$  and  $1150\text{ cm}^{-1}$  were from vibrations of the ether-type and  $\beta$ -O-4. Bands at  $1020\text{ cm}^{-1}$  and over  $900\text{ cm}^{-1}$  corresponded to vibrations due to the  $\beta$ -glucoside linkages of the cellulose. Most of the above bands are present in all samples analyzed and are in agreement with earlier published reports (Kubovsky and Kacik 2009; Navarro *et al.* 2009; Dyminska *et al.* 2014).

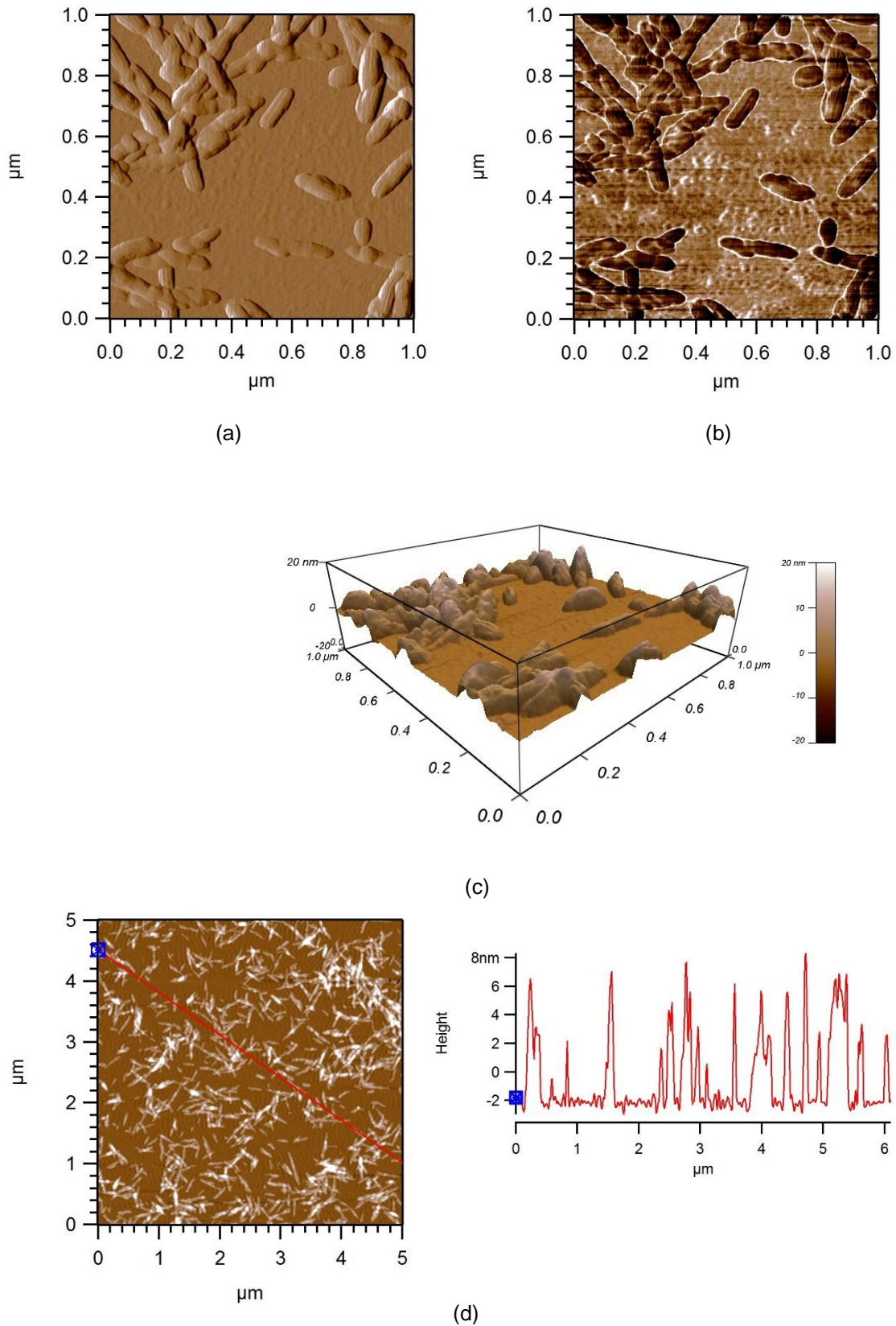


**Fig. 7.** AFM analysis images of NCCs obtained with experiment number 3: (a) amplitude, (b) phase, (c) 3D projection, and (d) section analysis graph

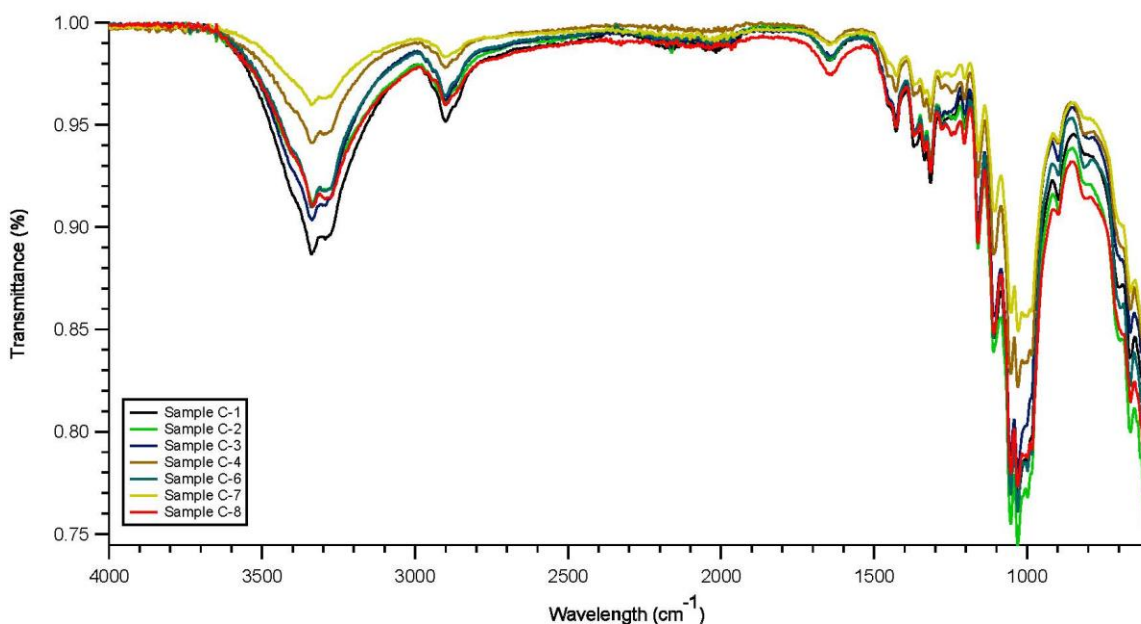


**Fig. 8.** Comparative ATR FTIR spectra of several films of NCCs, obtained from different controlled hydrolysis conditions considered in the experimental design

### Conductometric Analysis of NCCs

Figure 9 shows the graphs for the suspensions of NCCs obtained under the conditions of experiment numbers 1, 3, 7, and 8 (Table 2a and 2b) by conducting metric titrations using a strong acid with a strong base.

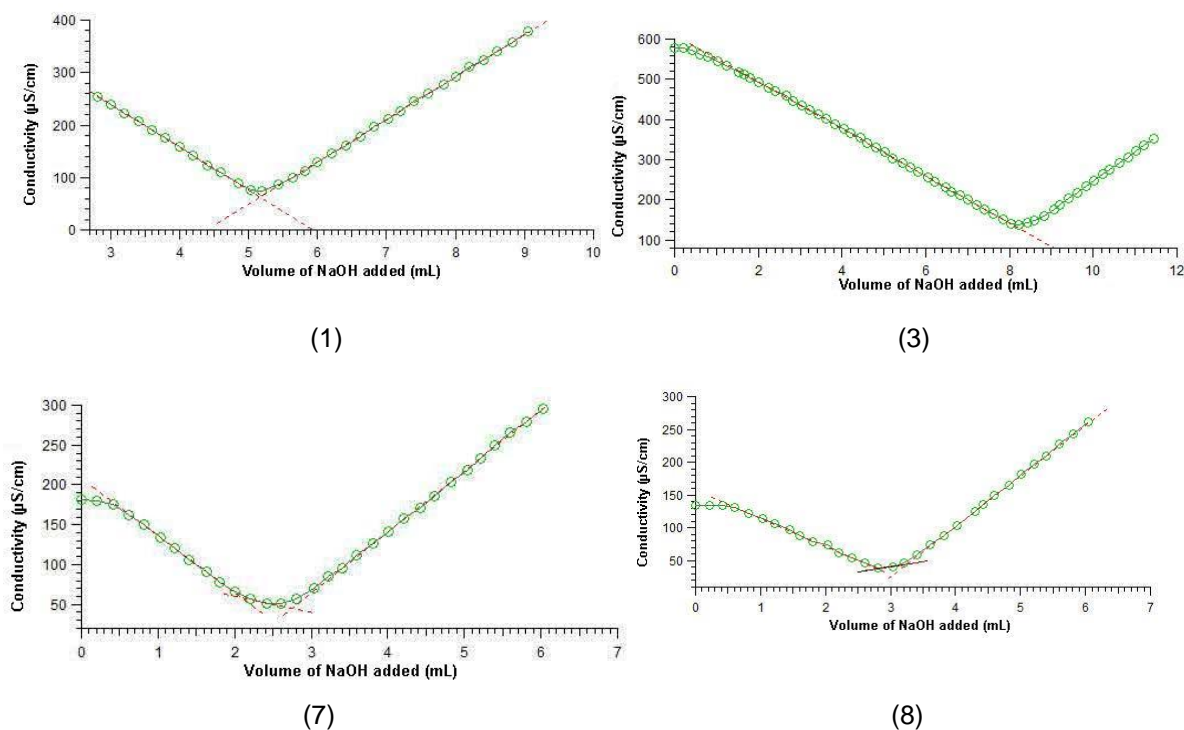


**Fig. 9.** Graphs resulting from the metric conductance evaluation of the NCC suspensions, obtained under the conditions of experiments numbers 1, 3, 7, and 8

With the addition of the titrant (NaOH) to the acid, the  $H^+$  of the acid would be consumed by the  $OH^-$  to form water. These  $H^+$  were progressively replaced by  $Na^+$  ions that had a lower ionic conductance than the  $H^+$  ions and, therefore, decreased the conductance of the solution.

After the equivalent point, the excess of  $Na^+$  and  $OH^-$  ions caused the conductance of the solution to increase. To calculate the mmol/g  $H_2SO_4$ , the NCC films were created to calculate the concentration (g/mL) of NCCs in each suspension. As shown in the figures, a similar trend was observed in all of the experiments, which indicated that when the various controlled acid hydrolysis conditions were used to obtain the NCCs, they all showed the presence of strong acid groups. This was due to the consequence of grafting on the surface of the NCCs of sulfate groups, *via* esterification, as has been reported by previous researchers (Araki *et al.* 1999; Roman and Winter 2004). Therefore, a statistical analysis of the experimental design applied to produce the NCCs was performed taking into account the concentration of acid groups per unit mass of NCCs in mmol/kg as the response variable.

This is illustrated in the 3D response surface graph shown in Fig. 10. In this figure, the colors indicate the ranges of load surface in mmol/kg of NCCs, and these types of graphs are very common types of graphs normally obtained in the study of the area surface chart generated by the experimental design in the Statgraphics program.

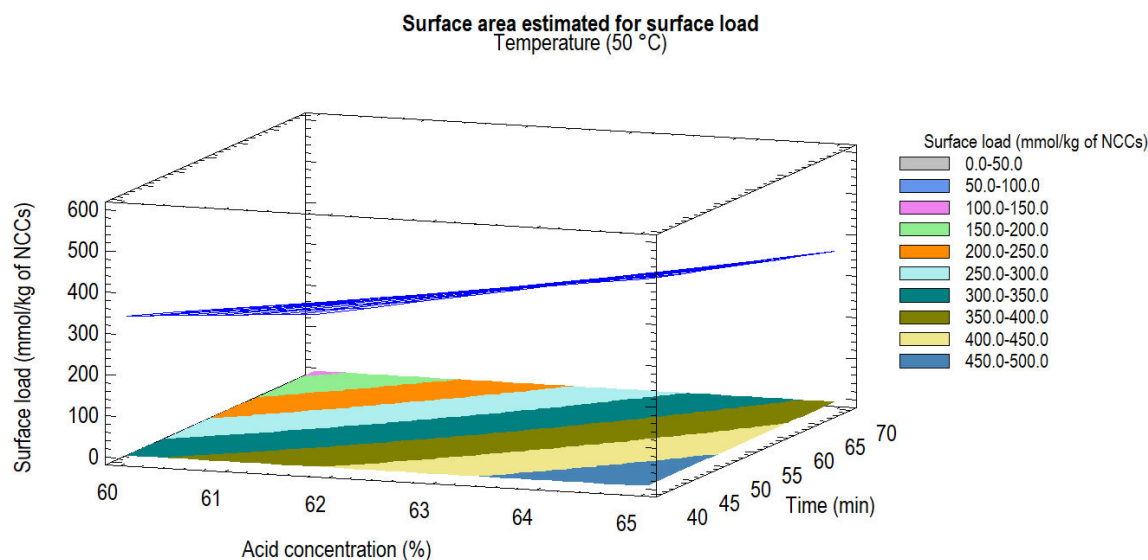


**Fig. 10.** Response surface of residual charge analysis in suspensions of NCCs, obtained under various acidic hydrolysis conditions controlled with  $H_2SO_4$ ; factors: acid concentration vs. treatment time

This figure suggests that, to generate suspensions of NCCs with a higher residual load of sulfate groups, the NCCs would have to be obtained using  $H_2SO_4$  concentrations of approximately 65% (highest design level for this factor) and short treatment times (40 min). In fact, this was achieved by generating a Pareto diagram (shows factors of greater influence in the analysis of the residual load of suspensions of NCCs) (data not shown) besides an experimental design already made. This indicates that the statistically significant factors are the concentration of the acid and the treatment time. Thus, to generate suspensions of NCCs with higher residual charge of sulphate groups, the

hydrolysis must be carried out at sulfuric acid concentrations of 65% and short treatment times (40 min).

## CONCLUSIONS

1. A new process was developed to obtain nanocellulose crystals using laser printed waste paper from a number of steps, which included deinking, use of high gain ultrasound with flotation, washing, and bleaching to isolate the material free of elemental chlorine.
2. It was possible to produce soluble grade cellulose, appropriate to obtain NCCs by the application of high gain ultrasound and bleaching. The latter resulted in sample with free elemental chlorine, a requirement to obtain NCCs.
3. These NCCs exhibited variable lengths (80 nm to 700 nm) depending on the acid hydrolysis conditions, as revealed by DLS and AFM studies. A statistical analysis of the experimental conditions revealed the most important factors that influenced the size and morphology of these NCCs were the concentration of H<sub>2</sub>SO<sub>4</sub> acid and the temperature at which the hydrolysis was conducted.
4. Although the maximum size of the particles was obtained with 60% acid at 40 °C and a treatment time of 50 min, it was necessary to use 65% acid and 40 min time of treatment to maximize the residual load of the sulfate groups.
5. Residual load evaluation data indicated that it was possible to obtain NCCs suspensions with variable loads that ranged between 130 mmol/kg to 570 mmol/kg of NCCs.
6. Produced NCCs exhibited highly desirable characteristics for cellulose derivatives, such as high values for whiteness (90.30% Elrepho),  $\alpha$ -cellulose contents (94.97%), and degrees of polymerization (731.34) besides chemical compositions similar to that of Whatman paper.

## ACKNOWLEDGEMENTS

The first author thanks the support of the National Council of Science and Technology (CONACYT) for the economic support for the development of this research and assistance to congresses, provided through projects INFR-2015-255323 and PDCPN2013-215773. The authors express their sincere thanks to the Chairman of the Department of Wood, Cellulose, and Paper of the University of Guadalajara for the interest in this study. The corresponding author (Dr. KGS) wishes to thank the Poornaprajna Institute of Scientific Research, Bangalore for their interest and encouragement in their publications, including this paper.

## REFERENCES CITED

Alén, R. (2000). "Structure and chemical composition of wood," in: *Forest Products Chemistry*, P. Stenius (ed.), Gummerus Printing, Jyväskylä, Finland, pp. 11-57.

- Alliot, M. L., and Avila, A. T. (2004). "Destintado de papel por flotación: influencia de los factores de forma," in: AIDIS Argentina. Desafíos ambientales y del saneamiento en el siglo XXI. Buenos Aires, AIDIS Argentina.
- Álvarez, O., and Abril, A. (2006). "Chemical characterization of recycled office paper with laser printing," in: *IV Ibero-American Congress of Research in Cellulose and Paper*, Santiago, Chile.
- Araki, J., Wada, M., and Kuga, S. (2001). "Steric stabilization of a cellulose microcrystal suspension by poly(ethylene glycol) grafting," *Langmuir* 17(1), 21-27. DOI: 10.1021/la001070m.
- Araki, J., Wada, M., Kuga, S., and Okano, T. (1999). "Influence of surface charge on viscosity behavior of cellulose microcrystal suspension," *J. Wood Sci.* 45, 258-261. DOI: <https://doi.org/10.1007/BF01177736>
- Beck-Candanedo, S., Roman, M., and Gray, D. G. (2005). "Effect of reaction conditions on the properties and behavior of wood cellulose nanocrystal suspensions," *Biomacromol.* 6(2), 1048-1054. DOI: 10.1021/bm049300p.
- Behin, J., Mikaniki, F., and Fadaei, Z. (2008). "Dissolving pulp (alpha-cellulose) from corn stalk by kraft process," *Iran. J. Chem. Eng.* 5(3), 14-28.
- Beneventi, D. B. C. (2000). "The mechanisms of flotation deinking and the role of fillers," *Prog. Paper Recycl.* 9, 77-85.
- Bian, H., Chen, L., Dai, H., and Zhu, J. Y. (2017). "Integrated production of lignin containing cellulose nanocrystals (LCNC) and nanofibrils (LCNF) using an easily recyclable di-carboxylic acid," *Carbohydr. Polym.* 167, 167-176. DOI: 10.1016/j.carbpol.2017.03.050.
- Bolio-López, G., Valadez-González, A., Veleza, L., and Andreeva, A. (2011). "Whiskers of cellulose from agro-industrial waste of bananas: Preparation and characterization," *Mexican J. Chem. Eng.* 10 (2), 291-299. [In Spanish].
- Bondeson, D., Aji, M. and Oksman, K. (2006). "Optimization of the isolation of nanocrystals from microcrystalline cellulose by acid hydrolysis," *Cellulose* 13:171-180. DOI: 10.1007/s10570-006-9061-4
- Camarero Espinosa, S., Kuhnt, T., Foster, E. J., and Weder, C. (2013). "Isolation of thermally stable cellulose nanocrystals by phosphoric acid hydrolysis," *Biomacromolecules* 14(4), 1223-1230. DOI: 10.1021/bm400219u.
- Chen, L., Wang, Q., Hirth, K., Baez, C., Agarwal, U. P., and Zhu, J. Y. (2015). "Tailoring the yield and characteristics of wood cellulose nanocrystals (CNC) using concentrated acid hydrolysis," *Cellulose* 22, 1753-1762. DOI 10.1007/s10570-015-0615-1.
- Chen, L., Zhu, J. Y., Baez, C., Kitin, P., and Elder, T. (2016). "Highly thermal-stable and functional cellulose nanocrystals and nanofibrils produced using fully recyclable organic acids," *Green Chem.* 18, 3835-3843. DOI: 10.1039/c6gc00687f.
- Desdelared (2012). <http://www.desdelared.com.mx/noticias/2012/2-opinion/0604-albino-0706141224>.
- De Souza Lima, M. M., Wong, J. T., Paillet, M., Borsali, R., and Pecora, R. (2002). "Translational and rotational dynamics of rodlike cellulose whiskers," *Langmuir* 19, 24-29. DOI: 10.1021/la020475z.
- Dong, X. M., Revol, J.-E., and Gray, D. G. (1998). "Effect of microcrystallite preparation conditions on the formation of colloid crystals of cellulose," *Cellulose* 5, 19-32. DOI: 10.1023/A:1009260511939,

- Dyminska, L., Gagor, A., Hanuza, J., Kulma, A., Preisner, M., Zuk, M., Szatkowski, M. and Szopa, T. (2014). "Spectroscopic characterization of genetically modified flax fibers," *J. Mol. Struct.* 1074, 321-329. DOI: 10.1016/j.molstruc.2014.06.013.
- Filson, P. B., Benjamin, E. D.-A., and Schweigler-Berry, D. (2009). "Enzymatic-mediated production of cellulose nanocrystals from recycled pulp," *Green Chem.* 11, 1808-1814. DOI: 10.1039/B915746H.
- Gaquere-Parker, A. C., Ahmed, A., Isola, T., Marong, B., Shacklady, C., Tchoua, P. 2009. "Temperature effect on an ultrasound-assisted paper de-inking process," *Ultrason. Sonochem.* 16, 698-703. DOI: 10.1016/j.ultsonch.2009.01.004
- Grossmann, H., Fröhlich, H., and Wanske, M. (2010). "The potential of ultrasound assisted deinking," in: *Tappi Peers Conference and 9<sup>th</sup> Research Forum on Recycling*, Norfolk, VA, USA, pp. 1682-1735.
- Guo, J., Guo, X., Wang, S., and Yin, Y. (2016). "Effects of ultrasonic treatment during acid hydrolysis on the yield, particle size and structure of cellulose nanocrystals," *Carbohydr. Polym.* 135, 248-255. DOI: 10.1016/j.carbpol.2015.08.068.
- Hamad, W. Y., and Hu, T. Q. (2010). "Structure-process-yield interrelations in nanocrystalline cellulose extraction," *The Canadian J. Chem. Engg.* 88(3), DOI: 10.1002/cjce.20298.
- Hossain, K. Z., Ahmed, I., Parsons, A., Scotchford, C., Walker, G., Thielemans, W., and Rudd, C. (2012). "Physico-chemical and mechanical properties of nanocomposites prepared using cellulose nanowhiskers and poly(lactic acid)," *J. Mater. Sci.* 47, 2675-2686. DOI: 10.1007/s10853-011-6093-4.
- Hu, Y., Tang, L., Lu, Q., and Huang, B. (2014). "Preparation of cellulose nanocrystals and carboxylated cellulose nanocrystals from borer powder of bamboo," *Cellulose* 21(3), 1611-1618. DOI: 10.1007/s10570-014-0236-0.
- ISO 11475 (2004). "Paper and board -- Determination of CIE whiteness, D65/10 degrees (outdoor daylight)," International Organization for Standardization, Geneva, Switzerland.
- Jonoobi, M., Harun, J., Mathew, A. P., Hussein, M. Z. B., and Oksman, K. (2010). "Preparation of cellulose nanofibers with hydrophobic surface characteristics," *Cellulose* 17, 299-307. DOI: 10.1007/s10570-009-9387-9.
- Kontturi, E., Meriluoto, A., Penttilä, P. A., Baccile, N., Malho, J.-M., Potthast, A., Rosenau, T., Ruokolainen, J., Serimaa, R., Laine, J., and Sixta, H. (2016). "Degradation and crystallization of cellulose in hydrogen chloride vapor for high-yield isolation of cellulose nanocrystals," *Angew. Chem. Int. Ed.* 55, 14455. DOI: 10.1002/anie.201606626.
- Kubovsky, I., and Kacik, F. (2009). "FT-IR study of maple wood changes due to CO<sub>2</sub> laser irradiation," *Cell. Chem. Techn.* 43, 235-240.
- Lee, C. K., Ibrahim, D., and Che Omar, I. (2013). "Enzymatic deinking of various types of waste paper: Efficiency and characteristics," *Proc. Biochem.* 48, 299-305. DOI: 10.1016/j.procbio.2012.12.015.
- Lorenz, M., Sattler, S., Reza, M., Bismarck, A., and Kontturi, E. (2017). "Cellulose nanocrystals by acid vapour: towards more effortless isolation of cellulose nanocrystals," *Faraday Discuss* 202, 315-330. DOI: 10.1039/c7fd00053g.
- Lu, P., and Hsieh, Y. L. (2012). "Preparation and characterization of cellulose nanocrystals from rice straw," *Carbohydr Polym* 87, 564-573.
- MacDonald, C. (2011). "Dissolving pulp draws renewed interest," *Pulp Pap.-Can.* 112 (3), 19-26.

- Matharu, A. S. De Melo, E. M. D., Remon, J., Wang, S., Abdulina, A., and Kontturi, E. (2018). "Processing of citrus nanostructured cellulose: A rigorous design-of-experiment study of the hydrothermal microwave-assisted selective scissoring process," *Chem. Sus. Chem* 11(8), 1344-1353. DOI: 10.1002/cssc.201702456
- Monte, M. C., Sánchez, M., Blanco, A., Negro, C., and Tijero, J. (2012). "Improving deposition tester to study adherent deposits in papermaking," *Chem. Eng. Res. Des.* 90, 1491-1499. DOI: 10.1016/j.cherd.2012.01.012
- Morán, J. I., Alvarez, V. A., Cyras, V. P., and Vázquez, A. (2008). "Extraction of cellulose and preparation of nanocellulose from sisal fibers," *Cellulose* 15, 149-159. DOI: 10.1007/s 10570-007-9145-9.
- Natthapong, P., and Kaenthong, S. (2018). "Regenerated cellulose from high alpha cellulose pulp of steam-exploded sugarcane bagasse," *J. Mater. Res. Technol.* 7(1), 55-65. DOI: 10.1016/j.jmrt.2017.04.003.
- Navarro, F., Davalos, F., Gonzalez-Cruz, R., Lopez-Dellamary, F., Manriquez, R., Turrado, J., and Ramos, J. (2009). "Sisal chemo-thermomechanical pulp paper with a strongly hydrophobic surface coating produced by a pentafluorophenyldimethylsilane cold plasma," *J. Appl. Polym. Sci.* 112, 479-488. DOI: 10.1002/app.29419
- Norman, J. C., Sell, N. J., and Danelski, M. (1994). "Deinking laser-print paper using ultrasound," *Tappi J. (USA)*. 77(3), 151-158.
- Pauck, W., Venditti, R., Pocock, J., and Andrew, J. (2012). "Using statistical experimental design techniques to determine the most effective variables for the control of the flotation deinking of mixed recycled paper grades," *Tappi J.* 2, 28-41.
- PTS-RH 010/87 (1987). "Testing of waste paper. Identification of the flotation deinkability of printed waste paper," Paper Technology Foundation (Papiertechnische Stiftung-PTS), Munich, Germany.
- Ramírez Casillas, R. (2004). *Destintado de Papel de Impresión Laser, Usando Ultrasonido [Deinking of Laser Printer by Applying an Ultrasonic Treatment]*, Master's Thesis, University of Guadalajara, Guadalajara, Jalisco. México.
- Ramírez, R., Ramos, J., and Turrado, J. (2004). "Deinking of laser printed paper by ultrasound, flotation and washing system," *Prog. Paper Recycl.* 13 (2), 29-36.
- Ramírez Valdovinos, E. (2013). "Destintado de papel de impresión láser aplicando secuencias con ultrasonido de acción intensiva y procesamiento magnético mecánico, orientado hacia la obtención de celulosa de alta pureza [Deinking of laser printing paper applying sequences with intensive action ultrasound and mechanical magnetic processing, oriented towards obtaining high purity cellulose], Postgraduation Seminar, Faculty of Forest Sciences, Autonomous University of Nuevo León, Guadalajara, Jalisco, Mexico.
- Roman, M., and Winter, W. T. (2004). "Effect of sulfate groups from sulfuric acid hydrolysis on the thermal degradation behavior of bacterial cellulose," *Biomacromol.* 5, 1671-1677. DOI: 10.1021/bm034519+
- Salminen, R., Reza, M., Pääkkönen, T., Peyre, J., and Kontturi, E. (2017). "TEMPO-mediated oxidation of microcrystalline cellulose: Limiting factors for cellulose nanocrystal yield," *Cellulose* 24, 1657-1667. DOI: 10.1007/s10570-017-1228-7.
- Samir, M. A. S. A., Alloin, F., Sanchez, J. Y., and Dufresne, A. (2004). "Cellulose nanocrystals reinforced poly(oxyethylene)," *Polym.* 45 (12), 4149-4157. DOI: 10.1016/j.polymer.2004.03.094
- Samira, E.-H., Nishiyama, Y., Putaux, J.-L., Heux, L., Dubreuil, F., and Rochas, C. (2008). "The shape and size distribution of crystalline nanoparticles prepared by acid

- hydrolysis of native cellulose,” *Biomacromolecules* 9, 57-65. DOI: 10.1021/bm700769p.
- Sell, N. J., and Norman, J. C. D. J. (1995). “Deinking secondary fiber using ultrasound,” *Prog. Paper Recycl.* 4(4), 28-34.
- Semarnat (2018). [http://www.semarnat.gob.mx/archivosanteriores/transparencia/transparenciafocalizada/residuos/Documents/directorio\\_residuos.pdf](http://www.semarnat.gob.mx/archivosanteriores/transparencia/transparenciafocalizada/residuos/Documents/directorio_residuos.pdf)
- Sixta, H. (ed.) (2006). *Handbook of Pulp*, Vol. 2, Ch. 8. WILEY-VCH Verlag GmbH & Co. KGaA, Weinheim.
- Šturcová, A., Davies, G. R., and Eichhorn, S. J. (2005). “Elastic modulus and stress-transfer properties of tunicate cellulose whiskers,” *Biomacromolecules* 6, 1055-1061. DOI: 10.1021/bm049291k.
- TAPPI T-203 om-93 (1993). “Alpha-, beta- and gamma-cellulose in pulp,” TAPPI Press, Atlanta, GA, USA.
- TAPPI T527 om-94 (1994). “Color of paper and paperboard (d/0, C/2,” TAPPI Press, Atlanta, GA, USA.
- TAPPI T-205 sp-95 (1995). “Forming handsheets for physical tests of pulp,” TAPPI Press, Atlanta, GA, USA.
- TAPPI T-205 om-07 (2007). “Color of paper and paperboard (d/0, C/2,” TAPPI Press, Atlanta, GA, USA.
- TAPPI T452 om-08 (2008). “Brightness of pulp, paper, and paperboard (directional reflectance at 457 nm),” TAPPI Press, Atlanta, GA, USA.
- TAPPI T218 sp-11 (2011). “Forming handsheets for reflectance testing of pulp (Büchner funnel procedure),” TAPPI Press, Atlanta, GA, USA.
- Tatsumi, D., Higashihara, T., Kawamura, S., and Matsumoto, T. (2000). “Ultrasonic treatment to improve the quality of recycled pulp fiber,” *J. Wood Sci.* 46, 405-409. DOI: 10.1007/BF00776405
- Testova, L., Borrega, M., Tolonen, L., Penttilä, P., Serimaa, R., Larsson, P., and Sixta, H. (2014). “Dissolving-grade birch pulps produced under various prehydrolysis intensities: quality, structure and applications,” *Cellulose* 21, 2007-2021. DOI: 10.1007/s10570-014-0182-x.
- Trache, D. M., Hazwan Hussin, M. K., Haafiz, M., and Thakur, V. K. (2017). “Recent progress in cellulose nanocrystals: Sources and production,” *Nanoscale* 9, 1763. DOI: 10.1039/c6nr09494e.
- Wang, Q., Zhao, X., and Zhu, J. Y. (2014). “Kinetics of strong acid hydrolysis of a bleached kraft pulp for producing cellulose nanocrystals (CNCs),” *Ind. Eng. Chem. Res.* 53(27), 11007-11014. DOI: 10.1021/ie501672m.
- Yu, H., Qin, Z., Liang, B., Liu, N., Zhou, Z., and Chen, L. (2013). “Facile extraction of thermally stable cellulose nanocrystals with a high yield of 93% through hydrochloric acid hydrolysis under hydrothermal conditions,” *J. Mater. Chem. A* 1(12), 3938-3944. DOI: 10.1039/c3ta01150j.

Article submitted: March 12, 2018; Peer review completed: May 24, 2018; Revised version received: July 18, 2018; Accepted: July 25, 2018; Published: August 14, 2018. DOI: 10.15376/biores.13.4.7404-7429